Research Paper
Computational Methods for Differential Equations
http://cmde.tabrizu.ac.ir
Vol. *, No. *, *, pp. 1-14
DOI:10.22034/cmde.2026.70289.3481

Solve linear singularly perturbed boundary value problems via domain decomposition and reproducing kernel collocation

X. L. Li[1] **and Fazhan Geng**[1,2,*]

[1]Department of Mathematics, Suzhou University of Technology, Changshu, Jiangsu 215500, PR China.

[2]School of Mathematics and Statistics, Hainan University, Haikou, Hainan 570228, PR China.

Abstract

We propose a uniformly convergent numerical scheme for singularly perturbed boundary value problems with a single boundary layer. The method combines the advantages of reproducing kernel theory with a domain decomposition strategy. Without loss of generality, we focus on problems exhibiting a left boundary layer, as the analysis for a right layer is mathematically equivalent. The original problem is first split into a boundary layer problem and a regular problem. The regular part is solved numerically using a high-order reproducing kernel collocation method on a uniform mesh, while the boundary layer part is resolved on a graded mesh using a similar high-order scheme. Both theoretical analysis and numerical experiments confirm the parameter-uniform convergence of the proposed approach.

Keywords. Reproducing kernel, Convection-diffusion problems, Boundary layers.

2010 Mathematics Subject Classification. 65L60, 34B15, 46E22.

1. Introduction

Consider the singular perturbation problem with boundary conditions:

$$\begin{cases} -\varepsilon u''(x) - b(x)u'(x) + c(x)u(x) = f(x), \ \ 0 < x < 1, \\ u(0) = \alpha_1, \ \ u(1) = \alpha_2, \end{cases} \tag{1.1}$$

where ε is a small positive parameter and $b(x) \geq \beta > 0$. We assume $b(x), c(x)$ and $f(x)$ are sufficiently smooth functions guaranteeing the existence of a unique solution to (1.1). Under the assumption above, a boundary layer occurs exclusively at the left endpoint $x = 0$.

Singularly perturbed problems play an important role in modeling various phenomena in science and engineering, such as fluid dynamics, chemical reactions, and optimal control. The defining feature of such problems is the presence of boundary or interior layers exhibiting sharp solution gradients. The direct application of classical numerical methods can not provide effective numerical solutions to singularly perturbed problems. Therefore, it is challenging to solve such problems effectively. Recent advances in numerical methods have yielded specialized techniques for effectively solving singularly perturbed problems. Natesan, Jayakumar and Vigo-Aguiar [13] proposed parameter uniform numerical approaches for singularly perturbed turning point problems by combining the piecewise uniform mesh and the classical finite-difference schemes. Andargie and Reddy [1, 2] developed fitted finite difference schemes for singular perturbation problems. Sharma et al. [9, 15, 16] presented numerical methods for singularly perturbed delay problems. Kadalbajoo et al. [11] introduced a collocation approach for singularly perturbed turning point problems. Podila et al. [14] proposed an initial value technique for singularly perturbed boundary value problems (SPBVPs). Cen et al. [4] presented an adaptive grid method for singularly perturbed problems with nonlocal conditions. Cheng and Mei [5] developed a local discontinuous Galerkin method for singularly perturbed problems. Jiang et al. [10] proposed a

Received: 18 November 2025; Accepted: 17 May 2026.
∗ Corresponding author. Email: fzg@cslg.edu.cn.

superconvergent numerical algorithm for singularly perturbed problems. Geng et al. [6–8, 17] developed several numerical algorithms for singularly perturbed problems by employing reproducing kernel theory. Kumar et al. [12] presented a boundary value method for linear SPBVPs.

The theory of reproducing kernels plays a significant role across multiple disciplines, including numerical analysis, differential equations, and statistical theory. In recent developments, novel reproducing kernel methods have been successfully developed for solving various classes of problems, encompassing ordinary differential equations boundary value problems, fractional order problems, and delay differential equations. Nevertheless, direct extension of the reproducing kernel methods to singularly perturbed differential equations presents significant theoretical and computational challenges. Building on reproducing kernel theory, Geng [6–8] established computational frameworks specifically designed for certain classes of singular perturbation problems. However, these methods are not parameter uniformly convergent. Compared to the works in [6–8], the present approach is parameter uniformly convergent. When ε decreases, comparable numerical accuracy can be maintained without increasing the number of nodes. Also, the present numerical approach achieves fourth-order convergence both in the regular and boundary layer regions. The method attains high numerical accuracy using relatively few nodes.

This study aims to design a parameter uniformly convergent numerical scheme for SPBVPs with boundary layer behavior, leveraging the theoretical framework of reproducing kernels.

The remainder of this paper is structured as follows: Section 2 presents the proposed numerical methodology for problem (1.1). The error and convergence analysis are provided in Section 3. Numerical experiments and results are discussed in Section 4. Some conclusions are included in the last section.

2. Parameter uniformly convergent methods

Let $r_1 = J_1\varepsilon$ and $r_2 = J_2\varepsilon$, where J_1 and J_2 are positive real numbers. It is required that $r_1 > r_2$ and the solution to problem (1.1) does not change rapidly on the interval $[r_2, r_1]$. Then the given interval $[0, 1]$ is divided into two overlapping subintervals $[0, r_1]$ and $[r_2, 1]$. The subinterval $[0, r_1]$ include the boundary layers region, and the solution on the subinterval $[r_2, 1]$ does not change rapidly.

Let $u(r_1) = \beta_1$ and $u(r_2) = \beta_2$, where β_1 and β_2 are undetermined constants. We solve the boundary value problems on subintervals $[0, r_1]$ and $[r_2, 1]$ respectively. And then the constants β_1 and β_2 are determined by the continuity of the approximate solutions.

Remark 2.1. The selection of parameters r_1 and r_2 has a certain degree of freedom, which is a advantage of the present approach. It is required that the solution on the subinterval $[r_2, 1]$ does not change rapidly and $J_1 < N_1$. The subinterval $[0, r_1]$ can be wider than the boundary layers region.

2.1 Solutions on the subinterval $[0, r_1]$

Define

$$Lu = -\varepsilon u''(x) - b(x)u'(x) + c(x)u(x).$$

Consider equation (1.1) restricted to the subinterval $[0, r_1]$:

$$\begin{cases} Lu = f(x), \ \ 0 < x < r_1, \\ u(0) = \alpha_1, \ \ u(r_1) = \beta_1. \end{cases} \tag{2.1}$$

In order to homogenize the boundary conditions of equation (2.1), we introduce a new unknown function

$$v(x) = u(x) - \rho(x), \tag{2.2}$$

where $\rho(x) = \gamma_1 + \gamma_2 x$ and satisfies $\rho(0) = \alpha_1, \ \rho(r_1) = \beta_1$.

To obtain the solution of (2.1), it only needs to solve the following problem

$$\begin{cases} Lv(x) = \overline{f}(x), \ \ 0 < x < r_1, \\ v(0) = 0, \ \ v(r_1) = 0, \end{cases} \tag{2.3}$$

where $\overline{f}(x) = f(x) - L\rho(x)$.

Now we introduce the method for solving problem (2.3).

Definition 2.2. Hilbert space H defined in E is called an reproducing kernel Hilbert space (RKHS) when a function $K : E \times E \longrightarrow R$ exists such that the following properties:
(1) For every $x \in E$, $K(\cdot, x) \in H$.
(2) $f(x) = (f, K(\cdot, x))_H$, $\forall f \in H, \forall x \in E$.

$K(x, y)$ is called the reproducing kernel (RK) of H. From [3], the RK is unique for a Hilbert space H.

Definition 2.3. $W^2[0, r_1] = \{u(x) \mid u'(x)$ is absolutely continuous, $u''(x) \in L^2[0, r_1]$, $u(0) = 0$, $u(r_1) = 0\}$. Its associated inner product takes the form:

$$(u(s), v(s))_2 = u(0)v(0) + u(r_1)v(r_1) + \int_0^{r_1} u''v''ds.$$

Theorem 2.4. *$W^2[0, r_1]$ is an RKHS with RK*

$$K_1(x, y) = \begin{cases} \tau_1(x, y), & y \le x, \\ \tau_1(y, x), & y > x, \end{cases} \tag{2.4}$$

where $\tau_1(x, y) = \frac{y\left(2r_1^2x - r_1\left(3x^2+y^2\right)+x\left(x^2+y^2\right)\right)}{6r_1}$.

The properties of $K_1(x, y)$:
(1) For every $y \in (0, r_1)$, $K_1(0, y) = K_1(r_1, y) = 0$.
(2) For every $y \in (0, r_1)$, $K_1(\cdot, y) \in C^2[0, r_1]$ and it is a piecewise polynomial.
(3) For every $y \in [0, r_1]$, $\frac{\partial K_1(\cdot, y)}{\partial y} \in C^1[0, r_1]$ and it is a piecewise polynomial.

By utilizing the RK $K_1(x, y)$ and selecting appropriate collocation points, we develop a novel collocation method that achieves uniform convergence with respect to the perturbation parameter. Let $X_{N_1} : 0 = x_1 < x_2 < \ldots < x_{N_1} = r_1$ be a partition of $[0, r_1]$, $x_l = (\frac{l-1}{N_1-1})^r r_1 (1 \le l \le N_1 - 1, r \ge 1)$, $\overline{h}_l = x_{l+1} - x_l$, $h_1 = \max\{\overline{h}_l\} = \overline{h}_{N_1-1}$ and $h = \frac{[(N_1-1)^r-(N_1-2)^r]J_1}{(N_1-1)^r}$. Clearly, $h_1 = h\varepsilon$. Let $\pi_l(x)$ denote the space of polynomials of degree at most l. Using the RK $K_1(\cdot, y)$, we construct basis functions $\{\varphi_l(x)\}$ for the approximation space. Put

$$\varphi_l(x) = \begin{cases} K_1(x, x_{l+1}), 1 \le l \le N_1 - 2, \\ \frac{\partial K_1(x,s)}{\partial s} \mid_{s=x_{l-N_1+2}}, N_1 - 1 \le l \le 2(N_1 - 1). \end{cases}$$

Let $S^1_{N_1} = Span\{\varphi_l(x), l = 1, 2, \cdots, 2N_1 - 2\}$. We find that

$$S^1_{N_1} = \{v(x) \in C^1[0, 1], v \mid_{[x_i, x_{i+1}]} \in \pi_3, i = 1, 2, \cdots, N_1 - 1\}.$$

Since $dim(S^1_{N_1}) = 2N_1 - 2$, the selection of $2N_1 - 2$ collocation nodes is necessary to maintain a well-posed approximation problem.
The collocation scheme employs the following nodal points:

$$X_{2N_1-2} = \{x_{li} = x_l + \mu_i h_1 \mid i = 1, 2, 1 \le l \le N_1 - 1\},$$

with $\mu_1 = \frac{3-\sqrt{3}}{6}$ and $\mu_2 = \frac{3+\sqrt{3}}{6}$ being the Gauss-Legendre quadrature points.
Our objective is to construct a collocation solution in the approximation space $S^1_{N_1}$ that converges to the true solution of (2.3).
We express the numerical approximation as the expansion:

$$v_{N_1}(x) = \sum_{l=1}^{2N_1-2} c_l \varphi_l(x). \tag{2.5}$$

Let $v_{N_1}(x)$ satisfy problem (2.3) at points in X_{2N_1-2}. This gives

$$Lv_{N_1}(s) = \sum_{l=1}^{2N_1-2} c_l L\varphi_l(s) = \overline{f}(s),\ s \in X_{2N_1-2}. \tag{2.6}$$

The value of $\{c_l\}$ can be computed by solving the resulting linear system of equations, after which the numerical solution $v_{N_1}(x)$ in equation (2.5) can be computed.

The approximation to the solution of (2.1) can be naturally derived from equation (2.2)

$$u_{N_1}(x) = v_{N_1}(x) + \rho(x). \tag{2.7}$$

2.2 Solutions on the subinterval $[r_2, 1]$

We solve equation (1.1) numerically on the subinterval $[r_2, 1]$:

$$\begin{cases} Lu = f(x), \ r_2 < x < 1, \\ u(r_2) = \beta_2, \ u(1) = \alpha_2. \end{cases} \tag{2.8}$$

To homogenize the boundary conditions of equation (2.8), let us introduce a new unknown function $w(x)$ defined by

$$w(x) = u(x) - \overline{\rho}(x), \tag{2.9}$$

where $\overline{\rho}(x) = \gamma_3 + \gamma_4 x$ and satisfies $\overline{\rho}(r_2) = \beta_2, \ \overline{\rho}(1) = \alpha_2$.

To obtain the solution of equation (2.8), it only needs to solve the following problem

$$\begin{cases} Lw(x) = g(x), \ r_2 < x < 1, \\ w(r_2) = 0, \ w(1) = 0, \end{cases} \tag{2.10}$$

where $g(x) = f(x) - L\overline{\rho}(x)$.

Next we introduce the method for solving problem (2.10).

Definition 2.5. $W^2[r_2, 1] = \{u(x) \mid u'(x)$ is absolutely continuous, $u''(x) \in L^2[r_2, 1], \ u(r_2) = 0, \ u(1) = 0\}$. Its associated inner product takes the form:

$$(u(y), v(y))_2 = u(r_2)v(r_2) + u(1)v(1) + \int_{r_2}^{1} u''v''dy.$$

Theorem 2.6. *$W^2[r_2, 1]$ is an RKHS with RK*

$$K_2(x, y) = \begin{cases} \tau_2(x, y), & y \le x, \\ \tau_2(y, x), & y > x, \end{cases} \tag{2.11}$$

where $\tau_2(x, y) = \frac{(x-1)y\left(r_2\left(x^2-2x+3y-2\right)-x^2+2x-y^2\right)}{6(r_2-1)}$.

The properties of $K_2(x, y)$:

(1) For every $y \in (r_2, 1)$, $K_2(r_2, y) = K_2(1, y) = 0$.

(2) For every $y \in (r_2, 1)$, $K_2(\cdot, y) \in C^2[r_2, 1]$ and it is a piecewise polynomial.

(3) For every $y \in [r_2, 1]$, $\frac{\partial K_2(\cdot, y)}{\partial y} \in C^1[r_2, 1]$ and it is a piecewise polynomial.

Let $X_{N_2} : r_2 = s_1 < s_2 < \ldots < s_{N_2} = 1$ be a partition of $[r_2, 1]$, $s_j = r_2 + (j-1)h_2$, $h_2 = \frac{1-r_2}{N_2-1}$. Using the reproducing kernel $K_2(\cdot, y)$, we construct basis functions $\{\phi_l(x)\}$ for the approximation space.

Put

$$\phi_l(x) = \begin{cases} K_2(x, s_{l+1}), 1 \le l \le N_2 - 2, \\ \frac{\partial K_2(x,y)}{\partial y} \mid_{y=s_{l-N_2+2}}, N_2 - 1 \le l \le 2(N_2 - 1). \end{cases}$$

Let $S^1_{N_2} = Span\{\phi_l(x), l = 1, 2, \cdots, 2N_2 - 2\}$. We find that

$$S^1_{N_2} = \{v(x) \in C^1[0, 1], v \mid_{[s_i, s_{i+1}]} \in \pi_3, i = 1, 2, \cdots, N_2 - 1\}.$$

Since $dim(S^1_{N_2}) = 2N_2 - 2$, the selection of $2N_2 - 2$ collocation nodes is necessary to maintain a well-posed approximation problem.

The collocation scheme employs the following nodal points:

$$X_{2N_2-2} = \{s_{li} = s_l + \mu_i h_2 \mid i = 1, 2, 1 \le l \le N_2 - 1\},$$

with $\mu_1 = \frac{3-\sqrt{3}}{6}$ and $\mu_2 = \frac{3+\sqrt{3}}{6}$ being the Gauss-Legendre quadrature points.
We seek the collocation approximation to the solution of problem (2.10) within the function space $S^1_{N_2}$.
The approximate solution takes the form

$$w_{N_2}(x) = \sum_{l=1}^{2N_2-2} \overline{c}_l \phi_l(x). \tag{2.12}$$

Let $w_{N_2}(x)$ satisfy problem (2.10) at points in X_{2N_2-2}. This gives

$$Lw_{N_2}(s) = \sum_{l=1}^{2N_2-2} \overline{c}_l L\phi_l(s) = g(s),\ s \in X_{2N_2-2}. \tag{2.13}$$

The value of $\{\overline{c}_l\}$ can be computed by solving the resulting linear system of equations, after which the numerical solution $w_{N_2}(x)$ in equation (2.13) can be computed.

The approximation to the solution of (2.8) can be naturally derived from equation (2.9)

$$u_{N_2}(x) = w_{N_2}(x) + \overline{\rho}(x). \tag{2.14}$$

2.3 Solutions on the entire interval $[0, 1]$

We determine the constants β_1, β_2 in $u_{N_1}(x)$ and $u_{N_2}(x)$ by virtue of the continuity of the solution $u(x)$ to (1.1) over the interval $[r_2, r_1]$. Take $\vartheta_1, \vartheta_2 \in [r_2, r_1]$, and let

$$u_{N_1}(\vartheta_1) = u_{N_2}(\vartheta_1),\ \ u_{N_1}(\vartheta_2) = u_{N_2}(\vartheta_2). \tag{2.15}$$

β_1 and β_2 can be obtained from the equations above.

Combining (2.7) and (2.14), we obtain the numerical solution to problem (1.1) over the complete interval $[0, 1]$ through

$$u_{N_1,N_2}(x) = \begin{cases} u_{N_1}(x), & 0 \le x \le r_1, \\ u_{N_2}(x), & r_1 < x \le 1. \end{cases} \tag{2.16}$$

3. Error and convergence analysis

Theorem 3.1. *If $b(x), c(x), f(x) \in C^4[0, r_1]$, then we have*

$$\| u_{N_1} - u \|_\infty \le C_1 h^4.$$

Proof. Let $G(x, s)$ denote the Green's function corresponding to the operator L under the boundary conditions specified in (2.3). We have,

$$v(x) = \int_0^{r_1} G(x, t)\overline{f}(t)dt.$$

It is worth noting that

$$\begin{aligned} v_{N_1}(x) - v(x) &= \textstyle\int_0^{r_1} G(x, s)[Lv_N(s) - Lv(s)]ds, \\ &= \textstyle\int_0^{r_1} G(x, s)[Lv_N(s) - \overline{f}(s)]ds. \end{aligned} \tag{3.1}$$

Let $Lv_{N_1}(s) = \overline{f}_{N_1}(s)$. This gives

$$v_{N_1}(x) - v(x) = \int_0^{r_1} G(x, s)[\overline{f}_{N_1}(s) - \overline{f}(s)]ds.$$

The subinterval $[x_l, x_{l+1}]$ contains two collocation points, x_{l1} and x_{l2}, from which we deduce that $Lv_{N_1}(x_{l1}) = \overline{f}(x_{l1})$ and $Lv_{N_1}(z_{l2}) = \overline{f}(x_{l2})$, that is, $\overline{f}_{N_1}(x_{l1}) = \overline{f}(x_{l1})$ and $\overline{f}_{N_1}(x_{l2}) = \overline{f}(x_{l2})$. Then

$$\begin{aligned} \overline{f}_{N_1}(s) - \overline{f}(s) &= \tfrac{\overline{f}''_{N_1}(\tau) - \overline{f}''(\tau)}{2}(s - x_{l1})(s - x_{l2}), \\ &\triangleq F''_l(\tau)(s - x_{l1})(s - x_{l2}), \end{aligned} \tag{3.2}$$

where $\tau \in [x_l, x_{l+1}]$. Let $H_l(x,s) = G(x,s)F_l''(\tau)$. Thus,

$$\int_{x_l}^{x_{l+1}} G(x,s)[\overline{f}_{N_1}(s) - \overline{f}(s)]ds = \int_{x_l}^{x_{l+1}} H_l(x,s)(s-x_{l1})(s-x_{l2})ds.$$

By performing a Taylor expansion of $H_l(x,s)$ centered at x_{l1}, we obtain

$$H_l(x,s) = H_l(x,x_{l1}) + \frac{\partial H_l}{\partial s}(x,x_{l1})(s-x_{l1}) + \frac{1}{2}\frac{\partial^2 H_l}{\partial s^2}(x,\tau)(s-x_{l1})^2.$$

Note that x_{l1} and x_{l2} are the Gauss nodes in $[x_l, x_{l+1}]$.
The Gaussian quadrature rule approximating $\int_{x_l}^{x_{l+1}} g(s)ds$ exactly integrates polynomials of degree up to 3. Consequently,

$$\int_{x_l}^{x_{l+1}} H_l(x,s)(s-x_{l1})(s-x_{l2})ds = \frac{1}{2}\int_{x_l}^{x_{l+1}} \frac{\partial^2 H_l}{\partial s^2}(x,\tau)(s-x_{l1})^3(s-x_{l2})ds. \tag{3.3}$$

On the boundary layer interval, one has

$$|v^{(j)}| = O(\varepsilon^{-j}).$$

Thus, we can find a constant $\beta > 0$ for which

$$\|\frac{\partial^2 H_l}{\partial s^2}(x,\overline{\tau})\|_\infty \le \beta\varepsilon^{-5}.$$

Then

$$|\int_{x_l}^{x_{l+1}} \frac{\partial^2 H_l}{\partial s^2}(s-z_{l1})^3(s-z_{l2})ds| \le \beta\varepsilon^{-5}h_1^5 = \beta\varepsilon^{-5}h^5\varepsilon^5 = \beta h^5. \tag{3.4}$$

Therefore,

$$\begin{aligned} \| v_{N_1} - v \|_\infty &\le \sum_{l=1}^{N_1-1} |\int_{x_l}^{x_{l+1}} H_l(x,\tau)(s-z_{l1})(s-z_{l2})ds|, \\ &\le (N_1-1)\beta h^5, \\ &\le C_1 h^4, \end{aligned}$$

where C_1 is a positive constant. It follows from (2.2) and (2.7) that

$$\| u_{N_1} - u \|_\infty \le C_1 h^4.$$

□

On the regular interval $[r_2, 1]$, one has

$$|w^{(j)}| \le C, j = 0,1,2,3,4,$$

where $C > 0$ is a constant independent of ε. By employing similar techniques to those used in proving Theorem 3.1, one gets the following result.

Theorem 3.2. *If $b(x), c(x), f(x) \in C^4[r_2, 1]$, then we have*

$$\| u_{N_2} - u \|_\infty \le C_2 h_2^4.$$

Theorem 3.3. *Under the assumption of Theorem 3.1 and 3.2, we have*

$$\| u_{N_1,N_2}(x) - u(x) \|_\infty \le \max\{C_1 h^4, C_2 h_2^4\}.$$

Remark 3.4. Since C_1, C_2 and h are independent of ε, and $h_2 = \frac{1}{N_2-1}$ as $\varepsilon \to 0$, it follows from Theorem 3.3 that the present approach can give same accuracy as $\varepsilon \to 0$.

Remark 3.5. Since the present method has a higher convergence order, the chosen values of N_1 and N_2 do not need to be large, leading to lower computational cost for the resulting linear systems (2.6) and (2.13).

Remark 3.6. The resulting linear systems (2.6) and (2.13) are dense, and we solve them using the command "LinearSolve" in soft Mathematica 12.0.

4. Numerical simulations

Example 4.1. Examine the following SPBVP

$$\begin{cases} -\varepsilon u''(x) - u'(x) + u(x) = f(x), \ \ 0 < x < 1, \\ u(0) = 3, u(1) = e + e^{-\frac{1}{\varepsilon}}, \end{cases}$$

with $f(x)$ selected to satisfy $u(x) = e^{-\frac{x}{\varepsilon}} + e^x - x + 1$. Taking $r = 1, r_1 = 25\varepsilon, r_2 = 23\varepsilon$, $N_1 = N_2 = 41, 81$, the maximum absolute errors (MAEs) obtained by the present algorithm for varying value of ε are provided in Table 1. Taking $r = 1$ and $N_1 = N_2 = 81$, the MAEs obtained by the present algorithm for different values of r_1 and r_2 are given in Table 2. Taking $r = 2$ and $N_1 = N_2 = 81$, the MAEs obtained by the present algorithm for different values of r_1 and r_2 are given in Table 3. Taking $J_1 = 25, J_2 = 23, r = 1$, the MAEs and convergence order on the boundary layer region $[0, r_1]$ are shown in Table 4. Taking $r = 2$, $N_1 = N_2 = 101$ and $r_1 = 33\varepsilon, r_2 = 31\varepsilon$, the absolute errors plots for $\varepsilon = 10^{-8}$ and $\varepsilon = 10^{-9}$ are shown in Figures 1–4. From Tables 1–4, we can see that the present approach is parameter uniformly convergent. Table 3 shows that the selection of r_1 and r_2 has a certain degree of freedom in the process of applying the present approach.

Table 1. Maximum absolute errors for varying parameter ε.

ε	$N_1 = N_2 = 41$	$N_1 = N_2 = 81$
10^{-5}	2.51×10^{-4}	2.08×10^{-5}
10^{-6}	2.54×10^{-4}	2.04×10^{-5}
10^{-7}	2.54×10^{-4}	2.04×10^{-5}
10^{-8}	2.54×10^{-4}	2.04×10^{-5}

Table 2. Maximum absolute errors with $r = 1$ and varying values of r_1, r_2.

ε	$r_1 = 25\varepsilon, r_2 = 23\varepsilon$	$r_1 = 27\varepsilon, r_2 = 27\varepsilon$	$r_1 = 29\varepsilon, r_2 = 27\varepsilon$	$r_1 = 31\varepsilon, r_2 = 29\varepsilon$
10^{-6}	2.04×10^{-5}	2.64×10^{-5}	3.44×10^{-5}	4.41×10^{-5}
10^{-7}	2.04×10^{-5}	2.64×10^{-5}	3.44×10^{-5}	4.41×10^{-5}
10^{-8}	2.04×10^{-5}	2.64×10^{-5}	3.44×10^{-5}	4.41×10^{-5}

Table 3. Maximum absolute errors with $r = 2$ and varying values of r_1, r_2.

ε	$r_1 = 25\varepsilon, r_2 = 23\varepsilon$	$r_1 = 27\varepsilon, r_2 = 25\varepsilon$	$r_1 = 29\varepsilon, r_2 = 27\varepsilon$	$r_1 = 31\varepsilon, r_2 = 29\varepsilon$
10^{-6}	5.21×10^{-6}	8.81×10^{-7}	3.28×10^{-7}	3.72×10^{-7}
10^{-7}	4.98×10^{-6}	9.24×10^{-7}	3.95×10^{-7}	3.79×10^{-7}
10^{-8}	4.95×10^{-6}	8.87×10^{-7}	4.16×10^{-7}	3.54×10^{-7}

Table 4. Maximum absolute errors and convergence order on $[0, r_1]$ with $r = 1$ and $\varepsilon = 10^{-6}, 10^{-8}$.

(N_1, N_2)	$MAE(\varepsilon = 10^{-6})$	Convergence order	$MAE(\varepsilon = 10^{-8})$	Convergence order
$(11, 11)$	2.80×10^{-2}	–	2.80×10^{-2}	–
$(21, 21)$	2.71×10^{-3}	3.37	2.71×10^{-3}	3.37
$(41, 41)$	2.53×10^{-4}	3.42	2.53×10^{-4}	3.42
$(81, 81)$	2.04×10^{-5}	3.63	2.04×10^{-5}	3.63

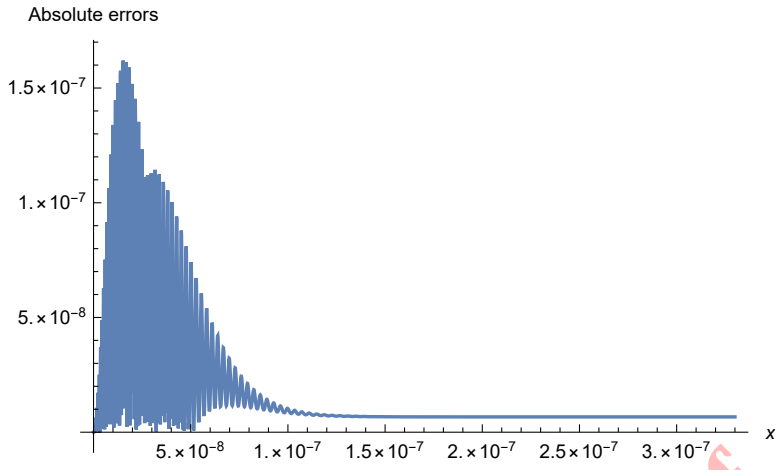

FIGURE 1. Error plots with $\varepsilon = 10^{-8}$ on $[0, r_1]$ for Example 4.1.

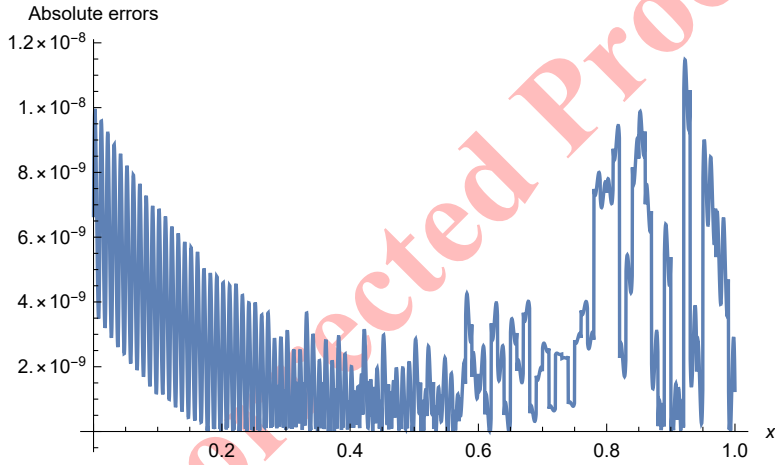

FIGURE 2. Error plots with $\varepsilon = 10^{-8}$ on $[r_1, 1]$ for Example 4.1.

Example 4.2. Solve the SPBVP consider in [8, 12]

$$\begin{cases} -\varepsilon u''(x) - u'(x) = f(x), \ \ 0 < x < 1, \\ u(0) = 0, u(1) = 1, \end{cases}$$

where $f(x) = -1 - 2x$. Its solution is

$$u(x) = \frac{(2\varepsilon - 1)(1 - e^{-\frac{x}{\varepsilon}})}{1 - e^{-\frac{1}{\varepsilon}}} + x(x + 1 - 2\varepsilon).$$

Taking $N_1 = N_2 = 101$ and $r_1 = 33\varepsilon, r_2 = 31\varepsilon$, Table 5 compares the absolute errors (AE) obtained using our method with the methods in [8, 12]. Taking $r = 1, r_1 = 25\varepsilon, r_2 = 23\varepsilon$, $N_1 = N_2 = 41, 81$, the MAEs obtained by the present algorithm for different value of ε are given in Table 6. Taking $r = 2$, $N_1 = N_2 = 101$ and $r_1 = 33\varepsilon, r_2 = 31\varepsilon$, the absolute errors plots for $\varepsilon = 10^{-7}$ and $\varepsilon = 10^{-9}$ are shown in Figures 5–8 The method in [8] combines the piecewise reproducing kernel method with the shooting method. The method in [12] is based on asymptotic expansion, stretching transformation, and the shooting method. Compared with [8, 12], the present method has a simpler implementation. Both the present method and the method in [12] require small computational workload.

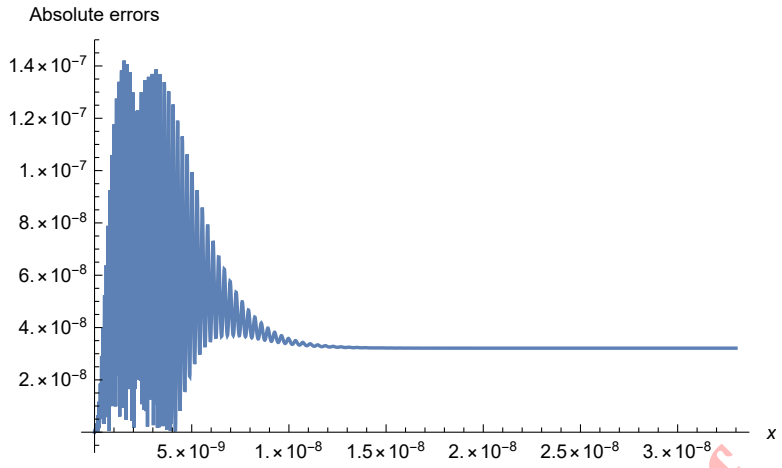

FIGURE 3. Error plots with $\varepsilon = 10^{-9}$ on $[0, r_1]$ for Example 4.1.

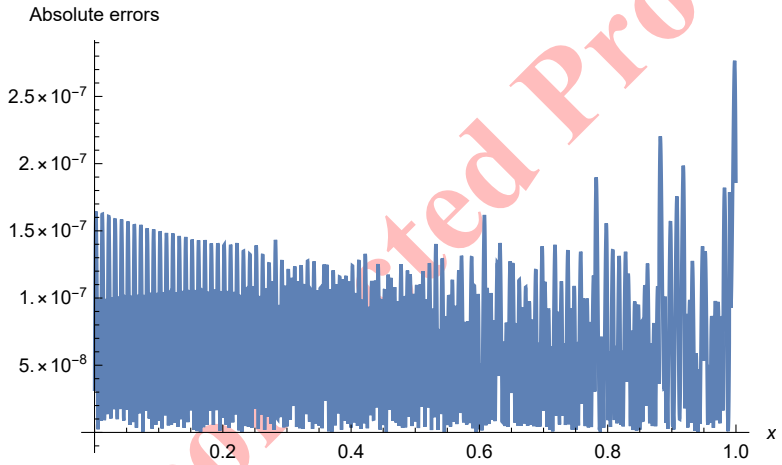

FIGURE 4. Error plots with $\varepsilon = 10^{-9}$ on $[r_1, 1]$ for Example 4.1.

TABLE 5. Numerical comparison for $\varepsilon = 10^{-4}$.

x	$u(x)$	AE in [12]	AE in [8]	AE (Present method with $r = 2$)	AE (Present method with $r = 1$)
0.000001	-0.00994718	–	3.67×10^{-7}	5.93×10^{-12}	3.62×10^{-7}
0.00001	-0.0951336	–	3.42×10^{-6}	3.76×10^{-9}	1.80×10^{-6}
0.0001	-0.631894	1.26×10^{-4}	1.46×10^{-5}	1.25×10^{-7}	5.89×10^{-6}
0.0010	-0.998754	1.99×10^{-4}	1.92×10^{-8}	6.09×10^{-9}	3.44×10^{-9}
0.0030	-0.996792	1.99×10^{-4}	1.98×10^{-10}	2.49×10^{-9}	9.98×10^{-9}
0.1000	-0.889820	1.80×10^{-4}	1.80×10^{-10}	1.74×10^{-9}	6.97×10^{-9}
0.5000	-0.249900	1.00×10^{-4}	1.02×10^{-10}	2.14×10^{-10}	8.58×10^{-10}
0.7000	0.1900600	6.00×10^{-5}	6.08×10^{-11}	3.93×10^{-11}	1.58×10^{-10}
0.9000	0.7100190	2.00×10^{-5}	2.04×10^{-11}	2.51×10^{-12}	1.62×10^{-12}

TABLE 6. Maximum absolute errors with $r = 1$ and varying values of ε.

ε	$N_1 = N_2 = 41$	$N_1 = N_2 = 81$
10^{-5}	2.54×10^{-4}	2.06×10^{-5}
10^{-6}	2.54×10^{-4}	2.06×10^{-5}
10^{-7}	2.54×10^{-4}	2.06×10^{-5}
10^{-8}	2.54×10^{-4}	2.06×10^{-5}

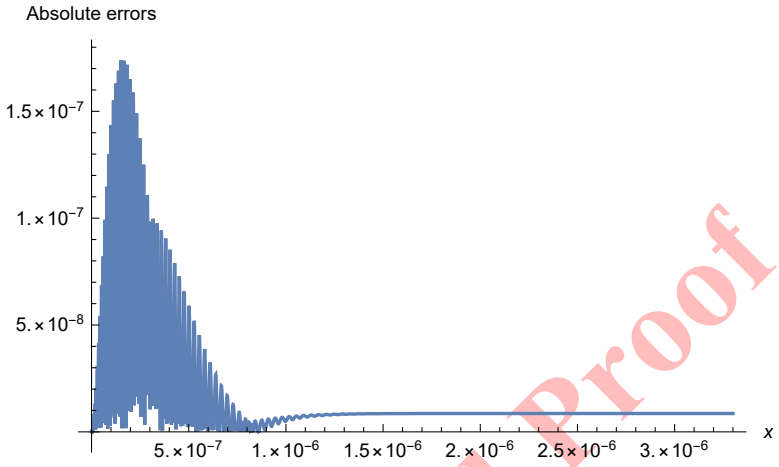

FIGURE 5. Error plots with $\varepsilon = 10^{-7}$ on $[0, r_1]$ for Example 4.2.

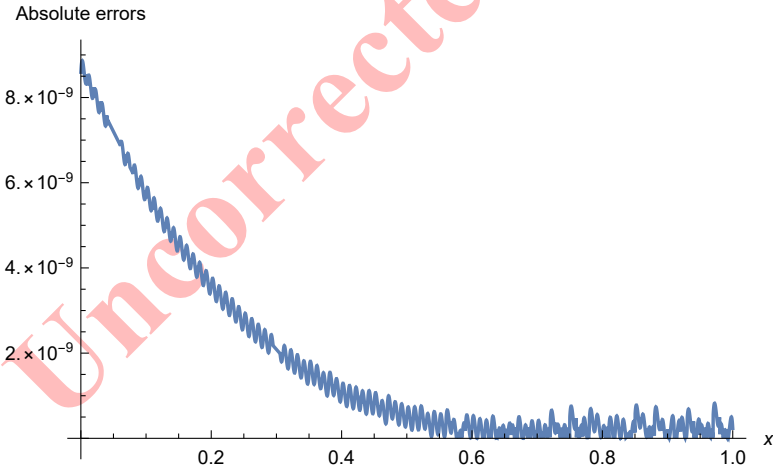

FIGURE 6. Error plots with $\varepsilon = 10^{-7}$ on $[r_1, 1]$ for Example 4.2.

Example 4.3. Solve the SPBVP as follows

$$\begin{cases} -\varepsilon u''(x) - (1 - \frac{x}{2})u'(x) + \frac{1}{2}u(x) = 0, \quad 0 < x < 1, \\ u(0) = 0, u(1) = 1, \end{cases}$$

Its solution is

$$u(x) = \frac{1}{2 - x} - \frac{1}{2}e^{-\frac{x - \frac{x^2}{4}}{\varepsilon}}.$$

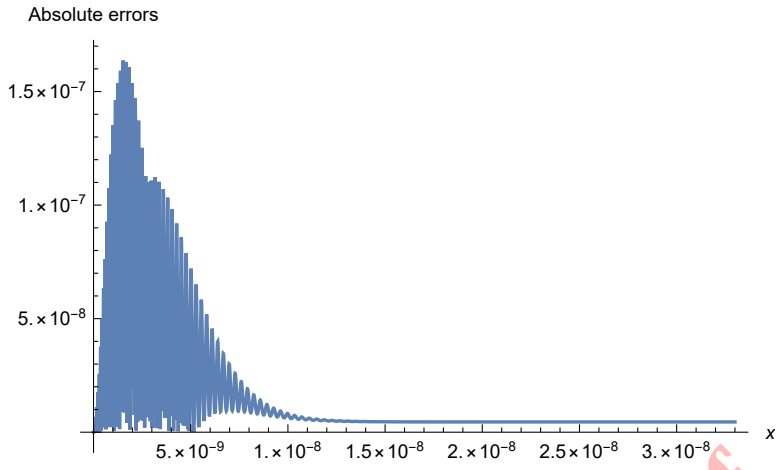

FIGURE 7. Error plots with $\varepsilon = 10^{-9}$ on $[0, r_1]$ for Example 4.2.

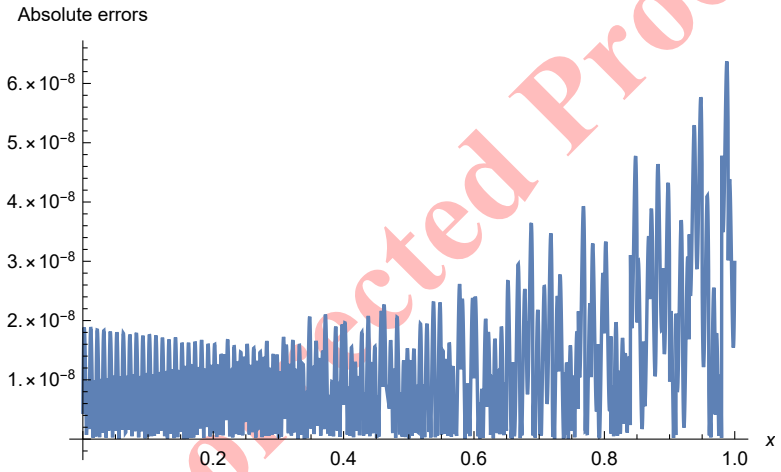

FIGURE 8. Error plots with $\varepsilon = 10^{-9}$ on $[r_1, 1]$ for Example 4.2.

Taking $r = 2$, $N_1 = N_2 = 101$ and $r_1 = 33\varepsilon, r_2 = 31\varepsilon$, the absolute errors plots on the entire interval $[0, 1]$ for $\varepsilon = 10^{-7}$ and $\varepsilon = 10^{-9}$ are shown in Figures 9 and 10.

Example 4.4. Solve the following SPBVP with right boundary layer

$$\begin{cases} -\varepsilon u''(x) + u'(x) + u(x) = f(x), \quad 0 < x < 1, \\ u(0) = 0, u(1) = \sin 1, \end{cases}$$

where $f(x)$ is selected such that the solution is

$$u(x) = \sin(x) e^{-(1-x)} \varepsilon.$$

Take $r = 2$, $N_1 = N_2 = 101$ and $r_1 = 1 - 31\varepsilon, r_2 = 1 - 33\varepsilon$. We take $x_i = \frac{i-1}{N1-1} r_1 (1 \le i \le N_1)$ and $x_{N_2+1-i} = r_2 + (1 - r_2)[1 - (\frac{i-1}{N_2-1})^r] (1 \le i \le N_2)$ on subintervals $[0, r_1]$ and $[r_2, 1]$ respectively. The absolute errors plots on the entire interval $[0, 1]$ for $\varepsilon = 10^{-5}$ and $\varepsilon = 10^{-7}$ are shown in Figures 11 and 12.

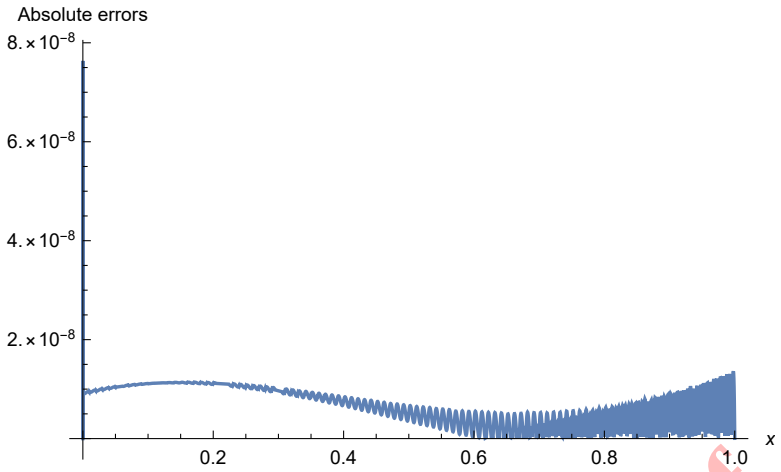

FIGURE 9. Error plots on $[0, 1]$ with $\varepsilon = 10^{-7}$ for Example 4.3.

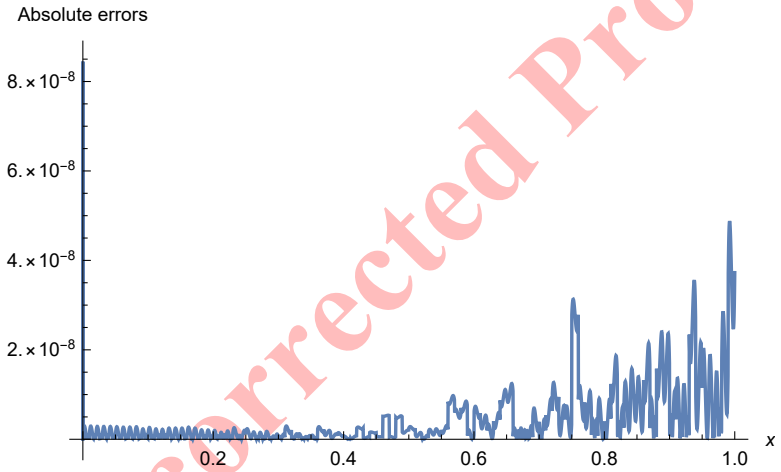

FIGURE 10. Error plots on $[0, 1]$ with $\varepsilon = 10^{-9}$ for Example 4.3.

5. Conclusion

We have presented a high-order, parameter-uniform numerical method for singularly perturbed boundary value problems with a left boundary layer. The method combines domain decomposition with reproducing kernel collocation, achieving robust convergence on both uniform and graded meshes, as confirmed by theoretical analysis and numerical experiments. The inherent flexibility in choosing parameters r_1 and r_2 further enhances its adaptability. Future work will aim to generalize this framework to time-dependent singularly perturbed partial differential equations.

Acknowledgment

Fazhan Geng was supported by the NSFC (Grant No.11271100) and China Postdoctoral Science Foundation (Grant No.2019M651765).

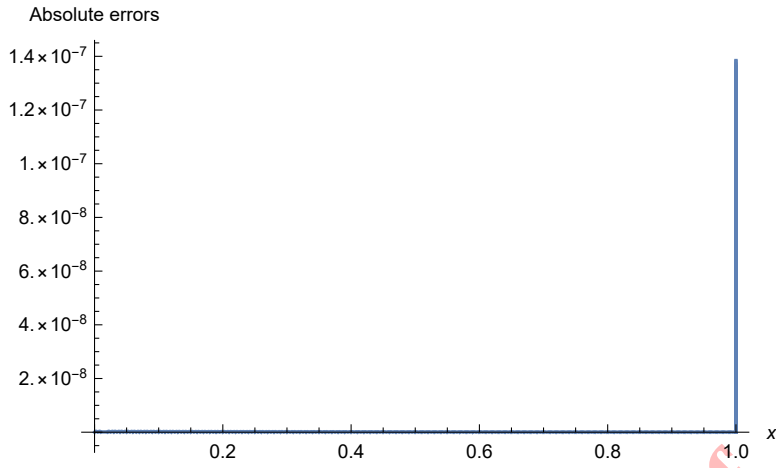

FIGURE 11. Error plots on $[0,1]$ with $\varepsilon = 10^{-5}$ for Example 4.4.

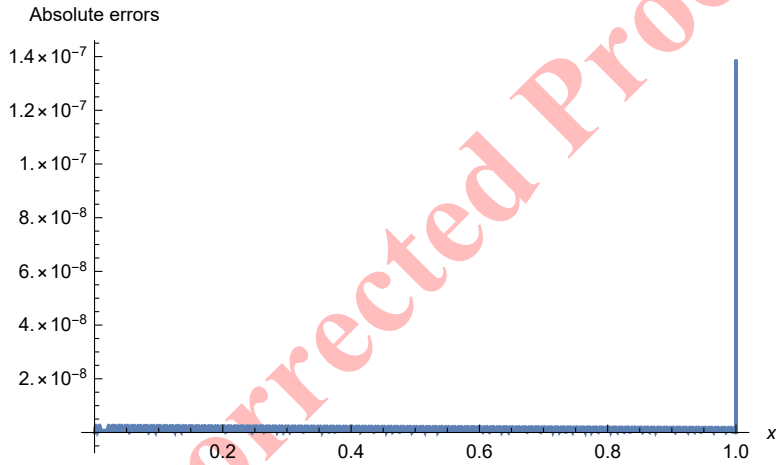

FIGURE 12. Error plots on $[0,1]$ with $\varepsilon = 10^{-7}$ for Example 4.4.

REFERENCES

[1] A. Andargie and U. N. Reddy, *Fitted fourth-order tridiagonal finite difference method for singular perturbation problems*, Appl. Math. Comput., *192* (2007) 90–100.

[2] A. Andargie and U. N. Reddy, *An exponentially fitted special second-order finite difference method for solving singular perturbation problems*, Appl. Math. Comput., *190* (2007), 1767–1782.

[3] N. Aronszajn, *Theory of reproducing kernels*, T. Am. Math. Soc., *68* (1950), 337–404.

[4] Z. D. Cen, L. B. Liu, and A. M. Xu, *A second-order adaptive grid method for a nonlinear singularly perturbed problem with an integral boundary condition*, J. Comput. Appl. Math. , *385* (2021), 113205.

[5] Y. Cheng and Y. J. Mei, *Analysis of generalised alternating local discontinuous Galerkin method on layer-adapted mesh for singularly perturbed problems*, Calcolo, *58* (2021), 52.

[6] F. Z. Geng and S. P. Qian, *A new numerical method for singularly perturbed turning point problems with two boundary layers based on reproducing kernel method*, Calcolo, *54* (2017), 515–526.

[7] F. Z. Geng, S. P. Qian, and S. Li, *A numerical method for singularly perturbed turning point problems with an interior layer*, J. Comput. Appl. Math., *255* (2014), 97–105.

[8] F. Z. Geng and Z. Q. Tang, *Piecewise shooting reproducing kernel method for linear singularly perturbed boundary value problems*, Appl. Math. Lett., *62* (2016), 1–8.
[9] J. Howlader, P. Mishra, and K. K. Sharma, *A parameter uniform orthogonal spline collocation method for time delay singularly perturbed semilinear reaction-diffusion problems*, J. Appl. Math. Comput., *71* (2025), 1077–1107.
[10] S. Jiang, X. Ding, and M. L. Sun, *Parameter-uniform superconvergence of multiscale computation for singular perturbation exhibiting twin boundary layers*, J. Appl. Anal. Comput., *13* (2023), 3330–3351.
[11] M. K. Kadalbajoo, P. Arora, and V. Gupta, *Collocation method using artificial viscosity for solving stiff singularly perturbed turning point problem having twin boundary layers*, Comput. Math. Appl., *61* (2011), 1595–1607.
[12] M. Kumar, H. K. Mishra, and P. Singh, *A boundary value approach for a class of linear singularly perturbed boundary value problems*, Adv. Eng. Softw., *40* (2009), 298–304.
[13] S. Natesan, J. Jayakumar, and J. Vigo-Aguiar, *Parameter uniform numerical method for singularly perturbed turning point problems exhibiting boundary layers*, J. Comput. Appl. Math., *158* (2003), 121–134.
[14] P. C. Podila, R. Mishra, and H. Ramos, *A numerical technique for solving singularly perturbed two-point boundary value problems*, Comput. Appl. Math., *43* (2024), 366.
[15] P. Rai and K. K. Sharma, *Numerical study of singularly perturbed differential-difference equation arising in the modeling of neuronal variability*, Comput. Math. Appl., *63* (2012), 118–132.
[16] P. Rai and K. K. Sharma, *Numerical analysis of singularly perturbed delay differential turning point problem*, Appl. Math. Comput., *218* (2011), 3483–3498.
[17] H. Sahihi, T. Allahviranloo, and S. Abbasbandy, *Computational method based on reproducing kernel for solving singularly perturbed differential-difference equations with a delay*, Appl. Math. Comput., *361* (2019), 583–598.